

DYNAMIC TENSILE BEHAVIOUR OF MAGNESIUM ALLOY AZ41 AT DIFFERENT STRAIN RATES AND TEMPERATURES

Gyan PRAKASH¹, N. K. SINGH², D. KUMAR³, P. CHANDEL⁴

Aim of the paper is to investigate the dynamic tensile behaviour of magnesium alloy AZ41 at different strain rates and temperatures. Quasi-static tests are performed on electromechanical universal testing machine at low strain rates (0.0001s⁻¹, 0.001s⁻¹, 0.01s⁻¹ and 0.1s⁻¹) and dynamic tests are conducted on split Hopkinson tensile bar setup at high strain rates (600s⁻¹, 850s⁻¹ and 1150s⁻¹) under tensile loads in room temperature 25°C. The quasi-static tensile tests are repeated at elevated temperatures (100°C, 150°C and 200°C) in constant strain rate 0.001s⁻¹. Fractographs (2000x) of broken tensile specimens at different temperatures are studied. The suitability of existing Cowper-Symonds and Johnson-Cook material models is examined.

Keywords: Magnesium alloy, strain rate sensitivity, split Hopkinson tensile bar and material models.

1. Introduction

Magnesium alloys are lightweight structural materials which are used for different engineering applications such as transportation, aviation, defence, electronic products etc. due to their high strength to density ratio. These alloys are readily available and have good heat dissipation, damping and manufacturing properties. It is necessary for the designers to understand the behaviour of the alloys under different loading conditions before designing its structures. There are many researchers who have investigated the mechanical characteristics of magnesium alloys. Influence of strain rates (0.0005-0.05s⁻¹) and temperatures (523-723K) on AZ31 magnesium alloy is observed by **Deng et al.** [1] and found the superplastic behaviour at higher temperatures ($\geq 673\text{K}$) and considerable strain hardening at lower temperatures (523K and 573K). **Maksoud et al.** [2] reported that the peak stress and hardness of the AZ31 alloy decrease while the volume fraction and size of dynamically recrystallized grains increase with decreasing strain rate (0.0001-0.01s⁻¹) and increasing deforming temperature (25-

¹ Research Scholar, National Institute of Technology Patna, India. Email: gpmitm46@gmail.com

² Asstt. Professor, National Institute of Technology Patna, India. Email: nilambersingh@nitp.ac.in

³ Scientist-C, TBRL, Sector-30, DRDO, Chandigarh, India. Email: davinder.84kumar@gmail.com

⁴ Scientist-E, TBRL, Sector-30, DRDO, Chandigarh, India. Email: chandel.drdo@gmail.com

404°C) under tensile loads. The uniaxial tensile tests are conducted by **Yin *et al.*** [3] to evaluate the warm deformation properties of hot-rolled AZ31 alloy at temperatures, 50-200°C and strain rates, 0.0014 - 0.14s⁻¹. The tensile behaviours of fatigued AZ31 magnesium alloy is studied by **Shu *et al.*** [4] and a comparison of flow behaviours of AZ31 and AZ80 magnesium alloys under tensile loads are carried out by **Qiao *et al.*** [5, 6] at varying strain rates (0.00005-0.02s⁻¹) and high temperatures (300-450°C). **Changjian *et al.*** [7] reported that the ultimate tensile strength and the ductility of the AZ31B alloy are much larger at high strain rates (193s⁻¹ and 1700s⁻¹) as compared to the low strain rate (0.000028s⁻¹). The fracture of this alloy exhibits a brittle feature. **Rodriguez *et al.*** [8] found that the mechanical properties of AZ31B alloy increase with increasing strain rate (0.0001-0.1s⁻¹) and decreasing temperature (25-300°C). The constitutive and failure behaviours of AZ31B magnesium alloy are studied by **Feng *et al.*** [9]. The microstructure analysis of AZ31B by **Ulacia *et al.*** [10] indicated that the deformation twins are more effective at high strain rates (500s⁻¹, 1000s⁻¹ and 1500s⁻¹) than in quasi-static strain rates (0.001s⁻¹ and 0.1s⁻¹). **Yu** [11] observed that the dynamic recrystallization and dislocation gliding mechanisms are the causes of the dynamic softening behaviour in AZ31B alloy at low strain rates (0.0005s⁻¹ to 0.01s⁻¹) and high temperatures (523K to 723K) under tensile loads.

Ahmad *et al.* [12] found that the ultimate tensile strength of the AZ91D magnesium alloy decreases by 35% and its fracture strength increases by 20% for an increase in temperature from 25°C to 250°C at strain rate 1500s⁻¹. **Sabokpa *et al.*** [13] investigated the hot ductility behaviour of AZ81 magnesium alloy in the temperature range from 250°C to 450°C and indicated a ductility drop at 400°C due to grain boundary sliding at different strain rates (0.0001s⁻¹ and 0.01s⁻¹). The as-cast ZA105 alloy has improved tensile properties compared to other high zinc-containing cast magnesium alloys (AZ91, ZA44, ZA75, ZA84, ZA104, ZA122, ZA104.5, ZAM105) as obtained by **Mohammed *et al.*** [14]. **Du *et al.*** [15] reported that the graphene nanoplatelets (GNPs) and the magnesium alloy ZK60 composites have enhanced tensile properties as compared with the alloy ZK60 at strain rate 0.003s⁻¹. The correlations of fatigue strength with tensile strength and hardness for AM50 magnesium alloy are proposed by **Marsavina *et al.*** [16]. **Wang *et al.*** [17] investigated the effects of Sc element on the microstructure and mechanical properties in the as-cast and as-rolled Mg-Sn-Zn alloys. **Garlea *et al.*** [18] studied the elastic mechanical properties and internal friction of two wrought magnesium alloys, AZ31B and ZK60A from 25°C to 450°C. The tensile crack initiation behavior of cast NZ30K magnesium alloy is studied by **Yue *et al.*** [19]. The present study is focused on the tensile behaviours of AZ41 magnesium alloy at different strain rates (0.0001-1150s⁻¹) and temperatures (25-200°C). The existing Cowper-Symonds and Johnson-Cook models with the estimated parameters predict the experimental results very well.

2. Materials and Specimens

The commercially available forged cylindrical rod of diameter 18mm and 4mm thick sheet of the magnesium alloy AZ41 are used to prepare specimens for tensile tests at different strain rates and temperatures. Specimens (Fig. 1a) of gauge length 40mm and diameter 10mm (middle section) are used for quasi-static (low strain rate) tensile tests on electromechanical universal testing machine whereas, the threaded specimens (Fig. 1b) of gauge length 13.4mm and diameter 5mm (middle section) are used for dynamic (high strain rates) tests on split Hopkinson tensile bar (SHTB) setup [20] in room temperature 25°C. Flat specimens (Fig. 1c) of gauge length 25mm and width 6mm as per ASTM standard are used for quasi-static tensile tests at high temperatures (100°C, 150°C and 200°C). Fig. 1d shows the fractured tensile specimens at different temperatures at strain rate 0.001s^{-1} . The chemical composition (wt.%) of the alloy as cylindrical rods is, Si: 0.014, Mn: 0.53, Fe: 0.001, Cu: 0.013, Al: 4.19, Zn: 0.89 and Mg: 94.362 whereas, the chemical composition (wt.%) of the alloy as sheet is, Si: 0.012, Mn: 0.32, Fe: 0.001, Cu: 0.011, Al: 3.991, Zn: 0.79 and Mg: 94.81.

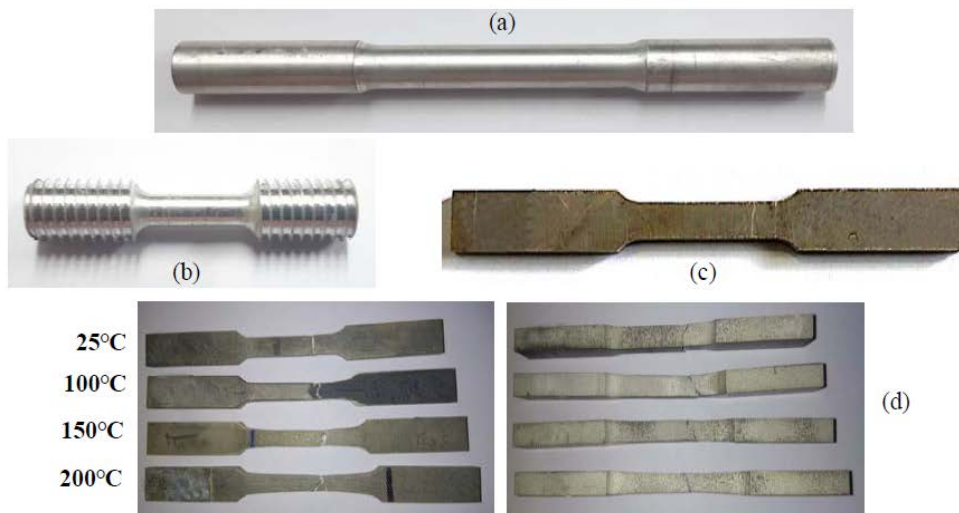


Fig. 1. Specimens (a) for quasi-static tensile tests at room temperature (b) for dynamic tensile tests at room temperature (c) for quasi-static tensile tests at high temperatures and (d) fractured at different temperatures under constant tensile loading rate, 0.001s^{-1} .

3. Results and discussion

Quasi-static and dynamic tensile behaviour of AZ41 magnesium alloy are discussed at different strain rates and temperatures. Quasi-static tests at low strain rates, 0.0001s^{-1} , 0.001s^{-1} , 0.01s^{-1} and 0.1s^{-1} are performed on electromechanical

universal testing machine of load bearing capacity 250 kN and dynamic tests at high strain rates 600s^{-1} , 850s^{-1} and 1150s^{-1} are conducted on split Hopkinson tensile bar setup in room temperature 25°C . The quasi-static test is repeated at high temperatures (100°C , 150°C and 200°C) on the same universal testing machine to understand the effects of temperature on flow stresses (the stresses to cause continued plastic deformation) of the alloy. The above experimental data are analyzed to obtain the stress-strain curves at different strain rates ($0.0001\text{-}1150\text{s}^{-1}$) and temperatures ($25\text{-}200^\circ\text{C}$). Three experiments are conducted at each strain rate/temperature and mean value of the mechanical properties is considered. The true stress-strain data are determined from experimentally obtained engineering stress-strain data using eqn. 2 of Ref. [21]. There is no need to measure the true area at any instant for calculating true stress as it has already been used in derivation of the formula of true stress. The engineering and true stress-strain curves at different strain rates under the room temperature are compared in Fig. 2a and Fig. 2b respectively. The yield stress is measured at 0.2% offset strain in the stress-strain curves of the alloy.

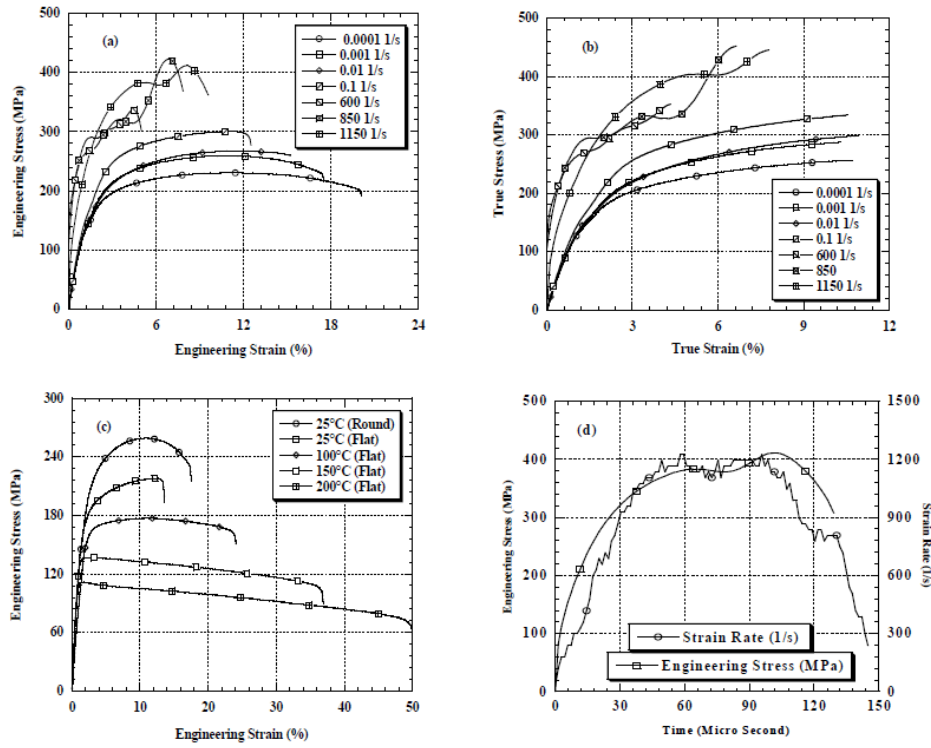


Fig. 2. Comparison of different curves (a) engineering stress-strain curves at room temperature (b) true stress-strain curves at room temperature (c) engineering stress-strain curves at different temperatures and (d) engineering stress and strain rate *versus* time curve at strain rate 1150s^{-1} in room temperature.

The experimental results of the alloy at various strain rates and temperatures are presented in Table 1. The AZ41 magnesium alloy shows positive sensitive [22] to strain rates i.e. the flow stress increases with increasing strain rate (0.0001-1150s⁻¹). At 1150s⁻¹, the alloy shows thermal softening and the ultimate tensile strength is almost similar to that at 850s⁻¹. On increasing the strain rate from 0.0001s⁻¹ to 1150s⁻¹, the true yield stress increases by approx. 77% and the true ultimate tensile strength increases by approx. 72%. The ductility of the alloy decreases with the increasing low strain rates (quasi-static) and decreasing high strain rates (dynamic) as per the total elongation in engineering stress-strain curves in respective strain rate levels (Table 1). It may be observed that ductility and toughness (area under stress-strain curve as shown in Table 1) at low strain rates (0.0001-0.1s⁻¹) is higher compared to that at high strain rates (600-1150s⁻¹).

Table 1
Experimental results of tensile tests at different strain rates and temperatures

Strain Rate (s ⁻¹)	Temperature (°C)	Engineering Stress-Strain Curves			Total Elongation (%)	True Stress-Strain Curves	
		Yield Stress (MPa)	UTS (MPa)	Toughness (Area under the stress-strain curve) MJ/m ³		Yield Stress (MPa)	UTS (MPa)
0.0001	25 (Round)	187 ± 2	232 ± 2	42 ± 0.64	20 ± 0.25	192 ± 2	261 ± 3
0.001		205 ± 1	257 ± 2	40 ± 0.70	17.5 ± 0.15	210 ± 1	284 ± 3
0.01		207 ± 2	265 ± 3	36 ± 0.55	15.2 ± 0.2	211 ± 2	296 ± 3
0.1		238 ± 3	297 ± 3	33 ± 0.46	12.5 ± 0.15	245 ± 3	330 ± 4
600		246 ± 3	340 ± 4	14 ± 0.28	5 ± 0.05	252 ± 3	355 ± 4
850		292 ± 3	418 ± 5	25 ± 0.44	8 ± 0.15	296 ± 3	456 ± 5
1150		335 ± 3	410 ± 4	32 ± 0.49	9.5 ± 0.15	344 ± 4	448 ± 4
0.001 (Flat)	25	177 ± 2	219 ± 2	26 ± 0.40	13.5 ± 0.2	181 ± 2	247 ± 3
	100	150 ± 2	176 ± 2	40 ± 0.65	24 ± 0.25	153 ± 2	195 ± 3
	150	131 ± 2	135 ± 2	45 ± 0.72	37 ± 0.3	132 ± 2	139 ± 2
	200	107 ± 1	111 ± 1	47 ± 0.76	50 ± 1	108 ± 1	113 ± 2

The engineering stress-strain curves at different temperatures (25°C, 100°C, 150°C and 200°C) are compared in Fig. 2c under constant strain rate 0.001s⁻¹. It is found that the flow stress of the alloy decreases with increasing temperature (25°C to 200°C) due to thermal softening. The strain hardening in round specimen prepared from as-received forged cylindrical rod is more as compared to that in flat specimen prepared from as-received flat sheet. The strain hardening in the flat specimen has decreased considerably at high temperatures (150°C and 200°C). Therefore, at higher temperatures ($\geq 150^\circ\text{C}$), a mixed brittle-ductile fracture mode in the specimen is expected. When the service temperature

increases from the room temperature 25°C to the high temperature 200°C, the true yield stress decreases by approx. 40% and the true ultimate strength decreases by approx. 54% (Table 1). The cross-sectional area at fracture decreases with increasing temperature as observed at strain rate 0.001s^{-1} (Fig. 1d). The ductility and toughness of the alloy increases with increasing temperature (25-200°C). Thus, in strain rate 0.001s^{-1} , the AZ41 magnesium alloy dissipates more energy (corresponds to area under stress-strain curve, Table 1) at high temperatures (100-200°C) as compared to that at room temperature 25°C. The engineering stress and strain rate *versus* time curve at 1150s^{-1} is given in Fig. 2d. The strain rate remains constant during plastic deformation of the alloy.

3.1 Fractography

The images of fracture surfaces of broken tensile specimens at different temperatures (25°C, 100°C, 150°C and 200°C) under constant strain rate 0.001s^{-1} are taken from scanning electron microscope (SEM) with magnification 2000x as shown in Fig. 3.

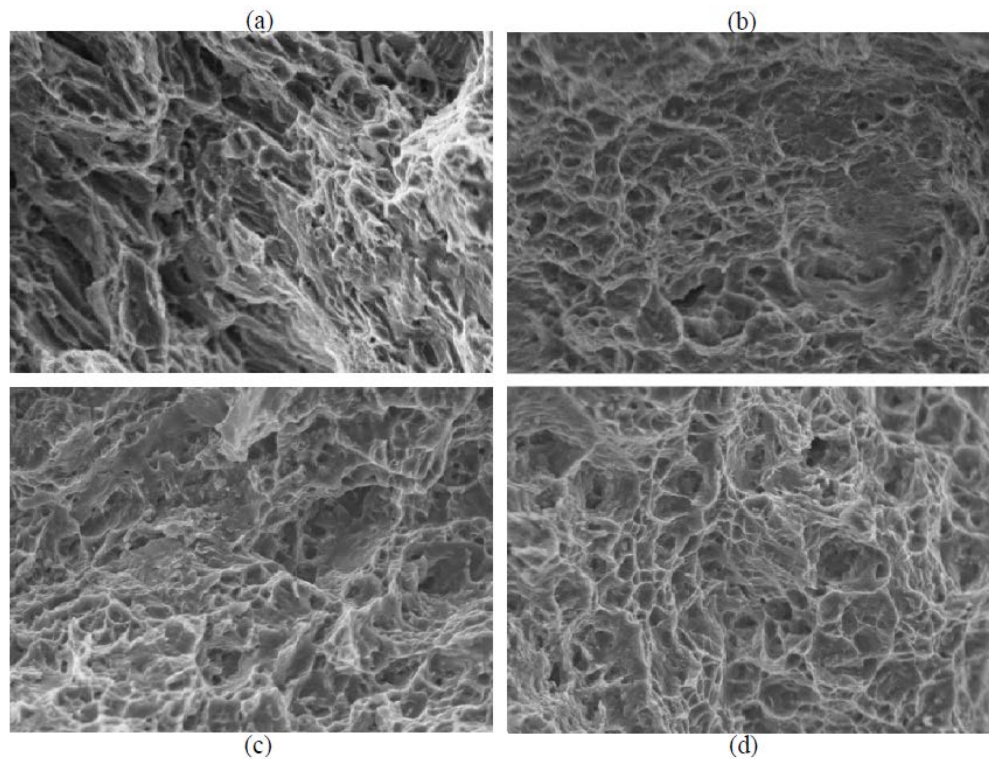


Fig. 3. SEM images (2000x) of fracture surfaces of broken flat specimens at temperatures (a) 25°C (b) 100°C (c) 150°C and (d) 200°C.

In room temperature (25°C), the alloy has cleavage fracture and some river patterns appear on the fractured surface. A small number of sallow dimples are also seen. At 100°C temperature, a combination of cleavage pattern and sallow dimples appear on the fracture surface of the specimen. At 150°C temperature, the cleavage pattern decreases and the number of dimples increases. In this case, the size of the dimples is increased. At 200°C temperature, the cleavage pattern is negligible and the fracture in the specimens is mainly due to the formation of dimples. The increased size of the dimples is responsible for large plastic deformation in the alloy. Thus, on increasing temperature from room temperature 25°C to the high temperature 200°C, the cleavage pattern decreases while the number and size of dimples increase. The fractographs reveal that the type of fracture changes from cleavage pattern dominant fracture to dimples pattern dominant fracture with increasing temperature (25-200°C).

3.2 Material Models

The material models are required to predict the experimental results under desired loading conditions where experiments are not possible to be performed. Here, the material coefficients of the existing Cowper-Symonds and Johnson-Cook models are evaluated from the experimental results through curve fitting method. It is found that the predicted results by these models match the experimental results very well. From literature [23], the Cowper-Symonds model can be written as:

$$\frac{\sigma_d}{\sigma_s} = 1 + \left(\frac{\dot{\varepsilon}}{D} \right)^{\frac{1}{q}} \quad (1)$$

Where, σ_d is true yield stress at high strain rate (dynamic), σ_s is true yield stress ($\dot{\varepsilon} = 0.0001\text{s}^{-1}$ as reference) at quasi-static strain rate that is equal to 192 MPa at 0.2% offset strain for AZ41 alloy, $\dot{\varepsilon}$ is the desired strain rate, $D = 1350.189$ and $q = 0.6853$ are material parameters calculated in Fig. 4a. The predicted results of Cowper-Symonds model fitted with the experimental data points in Fig. 4b.

From literature [24], the Johnson-Cook material model can be expressed as:

$$\sigma = [A + B\varepsilon_p^n] [1 + C \ln \dot{\varepsilon}^*] \quad (2)$$

Where, ε_p is the equivalent plastic strain; $\dot{\varepsilon}$ is the desired strain rate; $\dot{\varepsilon}_0$ ($= 0.0001\text{s}^{-1}$) is the reference strain rate, $\dot{\varepsilon}^* = \dot{\varepsilon}/\dot{\varepsilon}_0$ is the dimensionless plastic strain

rate. The equivalent plastic strain is considered as the plastic strain from yield point to the maximum point corresponding to the ultimate tensile strength in the true stress-strain curve obtained from experimental data at the reference strain rate 0.0001s^{-1} . A ($= 192$ MPa corresponding to 0.2% offset strain, Table 1) is true yield stress, B ($= 735.63$) and n ($= 1.0429$) are strain hardening parameters under quasi-static condition, and C is the strain rate sensitive parameter. The B, n and C parameters are determined by fitting the true plastic stress-strain curves from yield point (at 0.2% strain) to the maximum tensile stress. The C parameters at strain rate 600s^{-1} , 850s^{-1} and 1150s^{-1} are 0.029125, 0.037557 and 0.047076 respectively. The predicted results by Johnson-Cook model are compared with the experimental results in Fig. 5 at 0.0001s^{-1} and 1150s^{-1} .

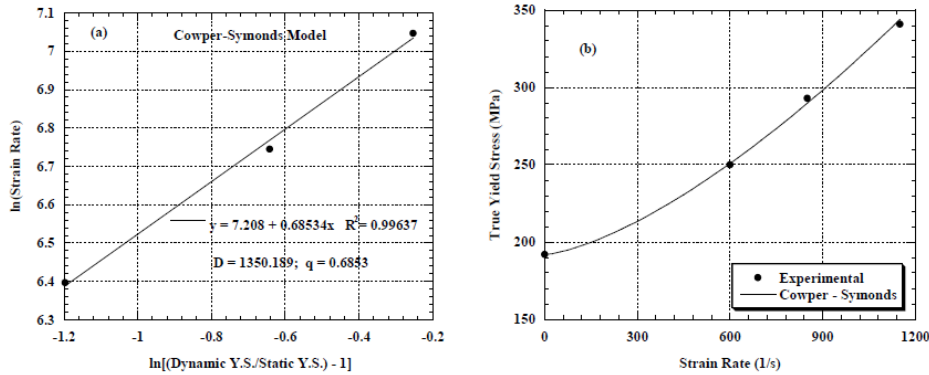


Fig. 4. Cowper-Symonds model (a) determination of material parameters and (b) fitting of predicted results with experimental data points.

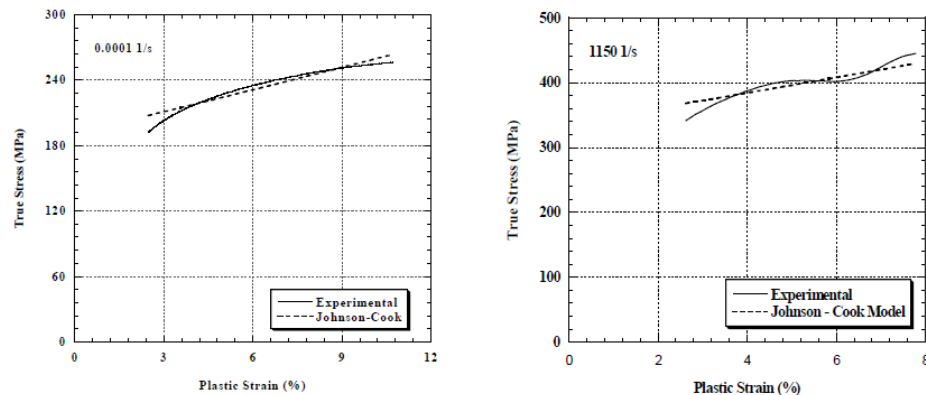


Fig. 5. Comparison of predicted results by Johnson-Cook model with the experimental results at strain rates, 0.0001s^{-1} and 1150s^{-1} .

4. Conclusions

The present investigation reveals that:

- The AZ41 magnesium alloy is positive sensitive to strain rate (0.0001-1150s⁻¹) under tensile loads. At 1150s⁻¹, the ultimate tensile strength of the alloy is almost similar to that at 850s⁻¹.
- On increasing temperature from room temperature 25°C to high temperature 200°C, the flow stress of the alloy decreases and ductility increases.
- The alloy has more ductility and toughness at low strain rates (0.0001-0.1s⁻¹) as compared to those at high strain rates (600-1150s⁻¹).
- With increasing temperature (25-200°C) dimple pattern fracture becomes dominant over cleavage pattern fracture.
- The existing Cowper-Symonds and Johnson-Cook models with estimated material parameters predict the flow stresses of the alloy in plastic zone very well.

R E F E R E N C E S

- [1]. *J. Deng, Y.C. Lin, S.S. Li, J. Chen and Y. Ding*, “Hot tensile deformation and fracture behaviors of AZ31 magnesium alloy”, Materials and Design, 49, 2013, 209–219.
- [2]. *I. A. Maksoud, H. Ahmed and J. Rodel*, “Investigation of the effect of strain rate and temperature on the deformability and microstructure evolution of AZ31 magnesium alloy”, Materials Science and Engineering A, 504, 2009, 40–48.
- [3]. *D.L. Yin, K.F. Zhang, G.F. Wang and W.B. Han*, “Warm deformation behavior of hot-rolled AZ31 Mg alloy”, Materials Science and Engineering A, 392, 2005, 320–325.
- [4]. *Y. Shu, X.Y. Zhang, J.P. Yu, L. Tan, R.S. Yin and Q. Liu*, “Tensile behaviors of fatigued AZ31 magnesium alloy”, Transactions of Nonferrous Metals Society of China, 28 (5), 2018, 896–901.
- [5]. *J. Qiao, Y. Wang and G. Shi*, “High temperature tensile behaviors of extruded and rolled AZ31 Mg alloy”, Transactions of Nonferrous Metals Society of China, 20, 2010, 540–544.
- [6]. *J. Qiao, F. Bian, M. He and Y. Wang*, “High temperature tensile deformation behavior of AZ80 magnesium alloy”, Transactions of Nonferrous Metals Society of China, 23, 2013, 2857–2862.
- [7]. *G. Changjian, W. Baolin, L. Fang, T. Wenwei and H. Zhenyu*, “Dynamic tensile behavior of AZ31B magnesium alloy at ultra-high strain rates”, Chinese Journal of Aeronautics, 28, 2, 2015, 593–599.
- [8]. *A.K. Rodriguez, G.A. Ayoub, B. Mansoor and A.A. Benzerga*, “Effect of strain rate and temperature on fracture of magnesium alloy AZ31B”, Acta Materialia, 112, 2016, 194–208.
- [9]. *F. Feng, S. Huang, Z. Meng, J. Hu, Y. Lei, M. Zhou and Z. Yang*, “A constitutive and fracture model for AZ31B magnesium alloy in the tensile state”, Materials Science & Engineering A, 594, 2014, 334–343.
- [10]. *I. Ulacia, C.P. Salisbury, I. Hurtado and M.J. Worswick*, “Tensile characterization and constitutive modeling of AZ31B magnesium alloy sheet over wide range of strain rates and temperatures”, Journal of Materials Processing Technology, 211, 2011, 830–839.

- [11]. *D.H. Yu*, “Modeling high-temperature tensile deformation behavior of AZ31B magnesium alloy considering strain effects”, *Materials and Design*, 51, 2013, 323–330.
- [12]. *I.R. Ahmad, X. Jing and D.W. Shu*, “Effect of temperature on the mechanical behavior of magnesium alloy AZ91D in the range between -30°C and 250°C”, *International Journal of Mechanical Sciences*, 86, 2014, 34–45.
- [13]. *O. Sabokpa, A. Z. Hanzaki and H. R. Abedi*, “An investigation into the hot ductility behavior of AZ81 magnesium alloy”, *Materials Science and Engineering A*, 550, 2012, 31–38.
- [14]. *S.M.A.K. Mohammed, D.J. Li, X.Q. Zeng and D.L. Chen*, “Cyclic deformation behavior of a high zinc-containing cast magnesium alloy”, *International Journal of Fatigue*, 125, 2019, 1–10.
- [15]. *X. Du, W. Du, Z. Wang, K. Liu and S. Li*, “Defects in graphene nanoplatelets and their interface behavior to reinforce magnesium alloys”, *Applied Surface Science*, 484, 2019, 414–423.
- [16]. *L. Marsavina, F. Iacoviello, L. D. Pirvulescu, V. D. Cocco and L. Rusu*. “Engineering prediction of fatigue strength for AM50 magnesium alloys”, *International Journal of Fatigue*, 127, 2019, 10-15.
- [17]. *P. Wang, E. Guo, X. Wang, H. Kang, Z. Chen, Z. Cao and T. Wang*, “The influence of Sc addition on microstructure and tensile mechanical properties of Mg–4.5Sn–5Zn alloys”, *Journal of Magnesium and Alloys*, (In Press).
- [18]. *E. Garlea, M. Radovic and P. K. Liaw*, “High-temperature dependency of elastic mechanical behavior of two wrought magnesium alloys AZ31B and ZK60A studied by resonant ultrasound spectroscopy”, *Materials Science and Engineering A*, 758, 2019, 86-95.
- [19]. *H. Yue, P. Fu, Z. Li and L. Peng*, “Tensile crack initiation behavior of cast Mg–3Nd–0.2Zn–0.5Zr magnesium alloy”, *Materials Science and Engineering A*, 673, 2016, 458-466.
- [20]. *P. Sharma, P. Chandel, V. Bhardwaj, M. Singh and P. Mahajan*, “Ballistic impact response of high strength aluminium alloy 2014-T652 subjected to rigid and deformable projectiles”, *Thin Walled Structures*, 126, 2018, 205-219.
- [21]. *N. K. Singh, E. Cadoni, M. K. Singha and N. K. Gupta*, “Dynamic Tensile and Compressive Behaviors of Mild Steel at Wide Range of Strain Rates”, *J. Eng. Mech.*, 139(9), 2013, 1197-1206.
- [22]. *S. Liu, S. Wang, L. Ye, Y. Deng and X. Zhang*, “Flow behavior and microstructure evolution of 7055 aluminum alloy impacted at high strain rates”, *Materials Science & Engineering A*, 677, 2016, 203–210.
- [23]. *G.R. Cowper and P.S. Symonds*, “Strain hardening and strain-rate effects in the impact loading of cantilever beams”, *Brown University Division of Applied Mathematics Report No. 28*.
- [24]. *G.R. Johnson and W. H. A. Cook*, “A Constitutive model and data for metals subjected to large strains, high strain rates and high temperatures”, *Proceedings of 7th Int. Symposium on Ballistics*, 541-547.